www.americanjir.com

ScientificScholar®
Knowledge is power
Publisher of Scientific Journals

American Journal of Interventional Radiology

Original Research *Interventional Oncology*

Percutaneous microwave ablation of a transgenic large animal porcine liver tumor model after intra-arterial embolization

Samuel L. Rice[1], Sagine Berry-Tony[2], Jamaal Benjamin[1], Fernando Gómez Muñoz[3], Mhd. Wisam Alnablsi[1], Regina Beets-Tan[3]

[1]Department of Radiology, UT Southwestern Medical Center, Dallas, Texas, [2]Department of Radiology, Mallinckrodt Institute of Radiology at Barnes-Jewish Hospital St. Louis, Missouri, United States, [3]Department of Radiology, Netherlands Cancer Institute-Antoni van Leeuwenhoekziekenhuis, Amsterdam, Netherlands.

***Corresponding author:**
Samuel L. Rice,
Department of Radiology, UT Southwestern Medical Center, Dallas, Texas, United States.

samuel.rice@utsouthwestern.edu

Received: 03 August 2024
Accepted: 22 October 2024
Published: 25 November 2024

DOI
10.25259/AJIR_36_2024

Quick Response Code:

ABSTRACT

Objectives: Percutaneous ablation with microwave ablation (MWA) successfully treats hepatic tumors (HTs) up to 3 cm in size when appropriate margins are achieved. MWA is limited when treating larger HT due to the disbursement of heat from adjacent tissue and vasculature. Embolization before MWA can achieve a larger ablation zone (AZ); however, no evaluation has been performed to assess the influence of proximal or distal embolization on AZ.

Material and Methods: Using a transgenic porcine liver tumor model, angiography and embolization of HT were performed with lipiodol or different-sized particles, ranging from 40 to 1200 μm to complete vascular occlusion followed by MWA for 4 min at 65 watts with subsequent *ex vivo* assessment of AZ.

Results: AZ volume using 40 μm, 100 μm, and 300–500 μm microparticles were significantly larger than for the control, non-embolization group(mean ± standard deviation: 40 μm: 17.48 cm^3 ± 1.22, $P \leq 0.001$; 100 μm: 14.81 cm^3 ± 0.43, $P \leq 0.001$; and 300–500 μm: 12.16 cm^3 ± 0.8, $P \leq 0.001$ compared to 6.06 cm^3 ± 2.02 in the control group.

Conclusion: Distal embolization with smaller particles produced significantly larger AZ in an *in vivo* liver tumor when compared to no embolization control, lipiodol, or proximal large particle embolization.

Keywords: Bland embolization, Colorectal cancer, Hepatocellular carcinoma, Microwave ablation, Percutaneous ablation

INTRODUCTION

Primary hepatic tumors (HT), most commonly hepatocellular carcinoma (HCC) are the fourth leading cause of cancer mortality worldwide, resulting in about 782,000 deaths/year.[1] Secondary metastatic neoplasms commonly appear in the liver. Colorectal cancer (CRC) is the most prevalent secondary, metastatic cancer to the liver, with nearly half of the patients diagnosed eventually developing metastasis.[2] Secondary spread to the liver of neuroendocrine, breast, and melanoma is also common.[3-5]

For patients with limited hepatic disease, surgical resection (SR) is the gold-standard treatment, improving overall survival.[6] However, only 10–20% of patients with HT are surgical

candidates due to comorbidities precluding SR such as underlying hepatic dysfunction, portal hypertension, or cardiopulmonary disease.[7] Other factors precluding SR are tumor extent and location.[8] Percutaneous ablation (PA) has been established as a comparable minimally invasive local therapy with less complications and faster recovery compared to SR for lesions up to 3 cm.[9,10] A critical limitation to PA has been local tumor progression due to incomplete ablation zones (AZs) in larger HT. A clinical need exists to permit the successful treatment of larger HT with appropriate margins.

Radiofrequency ablation (RFA) induces thermal damage through high frequency alternating current, causing ionic oscillation and frictional heating. Constraints of RFA include a limited active heating zone measuring only a few millimeters, heat sink effect from adjacent vessels, and electrical impedance from tissue desiccation which limits thermal transmission.[11] Microwave ablation (MWA) has been created to overcome these disadvantages. Compared to RFA, the electromagnetic field of MWA creates higher temperature, improving thermal conductivity and thus tissue penetration. MWA is also less affected by tissue impedance, carbonization, and heat sink.[12,13] The addition of embolization in combination with MWA has been proposed as a means to potentiate PA by improving heat conductivity and counteracting the heat sink effect to create a larger and more homogeneous AZ suitable for treatment of HT larger than 4 cm. Several retrospective clinical evaluations of the combined therapy in small clinical cohorts have exhibited these principles and clinical benefit in patients.[14-16] At present, limited preclinical data are available to assist clinicians in optimizing this combination therapy.

Employing a large animal transgenic oncopig model of a HT that has previously been shown to express vascular perfusion similar to HCC and CRC, this manuscript presents an evaluation of how different embolization techniques before MWA can affect the size of the AZ.[17]

MATERIAL AND METHODS

The Institutional Animal Care and Use Committee approved all research procedures 2022-103088-USDA. Eight 9-week-old Oncopigs (transgenic pigs with Cre-inducible TP53R167H and KRASG12D mutations) with a mean body weight of 25 kg were obtained from Sus clinicals Inc. (Chicago, IL). The animals were allowed to acclimate to the animal facility for 5 days. Before any procedures, the animals were fasted for 12 h. Each pig was sedated with an intramuscular injection of solution containing ketamine hydrochloride, acepromazine, and atropine sulfate. Once the pig was anesthetized, an endotracheal tube was inserted, and anesthesia was maintained with isoflurane, nitrous oxide, and oxygen.

Tumor induction (*in situ* method)

Using real-time ultrasound (US) guidance, an 18-gauge coaxial core biopsy of the liver was obtained (Bard Mission, BD, Franklin Lakes, NJ). The 2 cm tissue sample was allowed to incubate at room temperature for 20 min with an adenoviral vector (10^9 pfu Ad5CMVCre, University of Iowa Viral Vector Core) in phosphate-buffered saline that contained 15 mM calcium chloride. Calcium chloride added to adenovirus in phosphate-buffered saline results in co-precipitation of adenovirus and calcium phosphate, which improves viral transduction. The virus carries the Cre recombinase gene and activates TP53R167H and KRASG12D expression. A slurry was fashioned from the 1 mL mixture and Gelatin sponge (Gelfoam, Pfizer, Kalamazoo, MI) using a 3-way stopcock; the mixture, containing virus, core biopsy, and gelatin, was injected percutaneously through the coaxial needle into three different liver lobes using US guidance. Sites were selected to be as far apart as possible, easy and safe to access, and deep enough to avoid leakage of injected material into the peritoneum or subcutaneous soft tissues.

Angiography and intra-arterial embolization

Femoral artery access was achieved with the placement of a 5 Fr vascular sheath utilizing Seldinger technique. Selective angiogram of the hepatic arteries (HA) supplying the HT was performed using a 5 Fr glide cobra catheter (Terumo Medical, Somerset NJ) and coaxial 2.4 Fr Prograt (Terumo Medical, Somerset NJ) microcatheter catheter. Tumor embolization mixture was injected slowly and intermittently under fluoroscopic monitoring; the injection was continued until complete filling of the vascular bed was achieved with the desired endpoint of 5 heartbeats vascular stasis. Embolization material used (1) Embozene (Varian Medical Systems, Palto Alto, CA) 40 and 100 μm; Embosphere (Meritt Medical, Jordan UT) 300-500 and 900-1200 μm. Microsphere particles were mixed with 15 cc Omnipaque (iohexol) (GE Healthcare, Chicago, IL) contrast material. (3) Lipiodol® (ethiodized oil) (Guerbet, Villepinte France) was used as a liquid embolic, as a 4:1 emulsion with normal saline.

MVA

Simulating clinical PA, US guidance identified the HT and a safe percutaneous path. MWA was performed using the 2.45-GHz NEUWAVE System and a single 15-gauge NEUWAVE PRXT antenna (NeuWave Medical, Inc., Madison, WI). Control group underwent MWA without prior embolization. Experimental groups underwent MWA immediately after embolization. In all animals, MWA was performed for 4 min with the power of 65 watts. In total, 20 tumor sites were treated. At the end of all ablation procedures, the animals were euthanized with an intravenous sodium pentobarbital

solution without recovery from anesthesia 30 min after the MWA.

Pathology

The livers were removed *en bloc* and fixed in 10% neutral-buffered formalin. AZ was externally identified by visual inspection and palpation. The visible ablated lesions were photographed. Empiric measurements of the AZ were performed with calipers by two separate observers in isolation from each other; the extent of the border of the AZ, a whitish inner zone with minimal abnormal outer zone which appeared reddish and was believed to be hemorrhage, was estimated by macroscopic changes based upon both visual and tactile tissue changes in the liver for each pathologic specimen. The outer hemorrhage was excluded as viability could not be visually confirmed. The diameter of the coagulated area was measured in three dimensions: First, the diameter along the track of insertion of the needle electrode was determined. Second, the diameter measured in the plane perpendicular to the track of insertion of the needle electrode and which ran at the tip of the needle electrode was determined. Third, the diameter in the same plane but perpendicular to the second diameter was determined. Volume of the ellipsoid was calculated using:

$$V = \frac{4}{3}\pi abc$$

Where a, b, and c are the measured radius of the AZ.

The livers were cut into 3–5 mm thin axial macroscopic slices. Sections through the MWA and through the non-ablated liver were embedded in paraffin blocks and sectioned at 5 μm thickness. Hematoxylin and eosin-stained sections were reviewed.

Statistical analysis

The volume and length (major and minor axis) were compared between the control and treatment groups. A Welch's two-tailed *t*-test was used for comparisons between the groups. A calculated $P < 0.05$ was considered to be significant. Statistics were performed using Prism software (Version 10, GraphPad, La Jolla, CA, USA).

RESULTS

Tumor inoculation

Tumor inoculation within the liver of the oncopig was successful in 20 out of 24 locations or 83.3%, after 20 days. The HT was measured with US, the tumor mass varied in size from 0.8 to 2.8 cm in the longest axis, and the tumor volumes were between 2.5 and 8.2 cm^3.

Angiography and embolization

Angiography and embolization were successful in 100% of the animals. Tumor embolization with calibrated particles or lipiodol was performed within the vessels supplying the tumor with the goal of complete embolization of the HT vasculature. Post-embolization real-time digital subtraction angiography demonstrated delayed forward flow of blood into the tumor with minimum 5 beat stasis within the vasculature supplying the tumor. The volume of particles needed to achieve this degree of embolization was variable, depending on the size of the vascular bed.

Percutaneous MVA

All ablations were successful, and no adverse events related to arterial access, embolization, or ablation requiring secondary restorative procedure or termination of the experiment were encountered during or immediately after the procedure, and the presence of these was monitored by the proceduralist physician and veterinary staff [Figure 1].

The volume (mean ± standard deviation) of the AZ after distal embolization with particle sizes of 40 μm was 17.48 cm^3 ± 1.22 cm^3 or 65% larger than the control (6.06 cm^3 ± 2.02 cm^3); 100 μm, 14.81 cm^3 ± 0.43 cm^3, 59% larger than control, and with 300–500 μm particles, 12.16 cm^3 ± 0.8 cm^3 or 50% larger than control group [Table 1]. The MWA volume of the 40 μm when compared to the AZ after embolization with 900–1200 μm and lipiodol AZ was significantly larger ($P \leq 0.001$ and <0.001, respectively).

The largest particles which provide a more proximal embolization and the liquid embolic did not create an AZ that was significantly larger than the control (900–1200 μm; 9.28 cm^3 ± 3.29 cm^3 and lipiodol 5.79 cm^3 ± 1.2 cm^3, $P = 0.287$, $P = 0.547$).

The AZ of the oncopig *in vivo* control group, without embolization, was found to be significantly smaller ($P \leq 0.001$) when compared to the proposed AZ from the NeuWave probe manufacturers' product material for 4 min at 65 watts (12.1 cm^3).

The AZ diameter along the long access was also significantly longer after embolization with 40 μm, 100 μm, and 300–500 μm particles, 4.5 cm ± 0.47 cm, 4.68 cm ± 0.06 cm, and 4.5 cm ± 0.1 cm ($P \leq 0.001$, <0.001, <0.001), respectively, compared to the length in the control group (3.56 cm ± 0.17 cm).

Pathology

On histopathologic examination, AZ from all groups exhibited the characteristic findings of coagulation necrosis. A greater degree of hemorrhage and sinusoidal congestion was seen

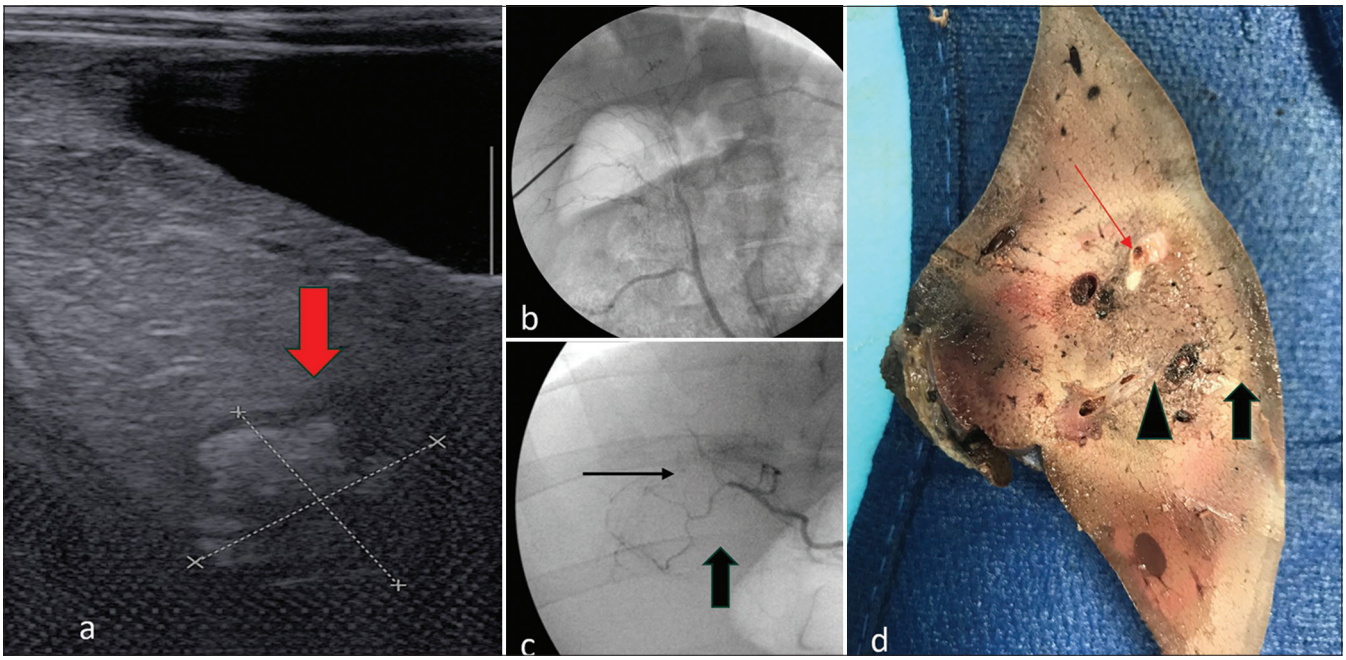

Figure 1: Liver tumor ablation in transgenic oncopig after embolization. (a) Ultrasound of the liver tumor (red arrow) Tumor is measured with calipers on Ultrasound Image. (b) Angiography of liver segment containing the liver tumor before embolization. (c) Post-embolization angiography with thin black arrowing showing tumor blush and thick black arrow identifying stasis of vascular flow within the tumor. (d) *Ex vivo* evaluation of the ablation zone after embolization. Black arrow is the non-charted coagulative zone, black triangle is the charred central portion, and the red arrow is the ablated tumor.

Table 1: Change in ablation zone size after pre-embolization with various material

Group	Ablation Zone (cm^3)		Length (cm)		Length (cm)	
	Volume	p=	Long axis	p=	Short axis	p=
Control (n=6)	6.06±2.02		3.56±0.17		2.29±0.19	
40 μm (n=8)	17.48±1.22	<0.001	4.5±0.47	<0.001	3.23±0.53	<0.001
100 μm (n=4)	14.81±0.43	<0.001	4.67±0.05	<0.001	3.17±0.11	<0.001
500 μm (n=3)	12.16±0.8	<0.001	4.5±0.1	<0.001	3.6±0.1	<0.001
1200 μm (n=4)	9.28±3.29	0.287	3.07±0.59	0.282	2.43±0.51	0.671
Lipiodol (n=3)	5.79±1.2	0.547	3.3±0.17	0.101	2.77±0.5	0.236
Manufacturer Insert	12.1		3.7		2.5	

at the periphery of the AZ in the control group compared with the particle embolization groups that had undergone a combined embolization/MWA treatment. Microspheres were noted within embolization/MWA zone, particularly within the central necrotic portion when smaller particles were used (40 and 100 μm); however, for the 900–1200 μm group, the majority of particles were in more central, larger diameter vessels or along the periphery of the AZ.

DISCUSSION

PA is an accepted local therapy for HT and can be employed with either curative intent or as palliative therapy.[6,18] A major limitation has been the maximum size of HT that can be completely treated, with studies reporting reliable local cure can only be achieved in HT <3 cm.[19-22] With all available thermal ablation techniques, the maximal size of the AZ that can be achieved is limited by the ability to conduct heat through the tumor and in adjacent liver tissue.

The present study, for the 1st time, attempted to combine transcatheter arterial embolization with MWA in a large animal tumor model, to specifically assess how the embolization particle size changes the AZ. A single ablation protocol of 65 watts and 4 min was performed in all HT independent of HT size; this protocol was chosen to compare the AZ size to the manufactures' estimation; ensure the AZ would remain entirely within the hepatic tissue for the most

accurate measurements; for an "apples to apples" comparison of the changes in the AZ for the different groups. Data obtained from HT embolization with particle size between 40 μm and 500 μm resulted in a significant increase in the size of the AZ when compared to MWA alone or to large particle embolization that generates a proximal, central blockage of the larger HA. This supports the hypothesis that distal embolization of the HT, at the tumor arterioles with smaller particles, results in an AZ volume, length, and width that is larger. Distal embolization results in the superior alleviation of the detrimental effects of heat sink at the periphery of the AZ, likely related to an inability of surrounding vessels within the adjacent hepatic segment to be recruited for passive dissipation of heat and energy conduction. When larger particles are used, a more proximal embolization occurs, similar to central arterial ligation, permitting hepatic segmental collateral vessels to be engaged, functioning to conduct heat away from the ablation probe. The size of the AZ volume after embolization with lipiodol is similar to no embolization, suggesting embolization with the liquid embolic lipiodol alone permits residual blood flow in the, incompletely obstructing the flow of blood through the HA when compared with particles.

Animal models are essential to the study of human tumors; the most commonly employed models are in small animals. Considerable limitations exist in the quality of data obtained when animals with major differences in genetics, anatomy, and physiology compared to humans are exploited for research, such as rodents. The transgenic oncopig model is a new orthotopic tumor model for human cancer. Pigs permit the use of the same equipment applied in clinical patients, and thus, the data are easily translatable to humans. The presence of a tumor within a liver is also an ideal imitation of clinical MWA as tumor tissue has a distinct characterization and matrix when compared to normal liver tissue; prior porcine studies have been in normal liver tissue. The HT vascularity in the oncopig model has previously been shown to produce some hypervascular and hypovascular tumors that are similar to either HCC or CRC liver metastasis and has been used to assess the transcatheter embolization procedure.[17]

When assessing MWA, the phenomenon of thermal convection exists only in an *in vivo* model. The presence of thermal convection results in the need for more energy to be delivered to reach a similar volume of AZ when compared to an *ex vivo* evaluation.[23] Testing the AZ in an *in vivo* model is essential to accurately evaluate the ablation procedure and translate these results into clinical practice. In this animal tumor model, an AZ that was significantly smaller was observed when compared to the manufactures' package insert of expected AZ volume for 65 watts and 4 min (12.1 cm^3); this is likely because most data obtained for studying PA AZ is performed in *ex vivo* organs without tumors.

Various tools are available to perform thermal PA, including RFA, cryoablation, and irreversible electroporation. PA with different modalities has previously been studied with or without embolization; however, this work has been in normal non-tumor-bearing animals. In addition, this study is crucial because it evaluated MWA whereas most previous experimental work has applied embolization with RFA. MWA has superior heating characteristics; thus, reliably achieving appropriate margins in HT >3 cm in combination with embolization was felt more probable.[24] A limited number of other groups have reported on embolization with PA but have applied different techniques to achieve arterial or portal embolization, which have included open vascular ligation as well as transcatheter procedures. Takamura *et al*. using MWA found that portal venous flow was most important to the diameter of the coagulation zone.[25] This is logical since the liver receives the majority of its blood supply from the portal vein, and thus, embolization of the portal vein would have a greater influence on the vascular heat sink compared to arterial embolization. The most common embolization technique studied has been using lipiodol and gelfoam followed by RFA, most of these studies found only a small, increase in the AZ, predominantly along the short axis diameter from the ablation probe; moreover, a shorter time to achieve the AZ was also observed.[26-29] Tanaka *et al*. in a normal pig studied ablation with calibrated particles before and after RFA and found smaller particle size significantly influenced the size of the AZ when performed before PA, not after.[30]

In an open procedure, dissimilar to clinical transcatheter embolization performed by interventional radiologists, ligation of the hepatic blood supply followed by RFA, Shibata *et al*. reported RFA produced a significantly larger and more spherical AZ.[31] An additional study assessing open, surgical MWA after clinical transcatheter embolization using 100–300 μm was completed and reported a significant increase in the area and diameter of the AZ after embolization, up to 60% that was specifically related to an increase in the peripheral zone. This study is comparable with the data obtained in our experiments that show a 65% increase when using 40 μm and 59% increase with 100 μm particles.[32]

Limitations to this study include the small number of ablations for each group. During the design of the examination, calculations were made to optimize the power of the study to achieve a statistically significant result, which was achieved; however, more data points would have improved the study and help to better characterize the specific changes certain embolization materials cause when combined with ablation. Due to certain logistical challenges posed by working with large animals at our institution, cross-sectional imaging was not obtained pre or post-ablation which would have provided *in vivo* data concerning tumor perfusion after embolization and an *in vivo* assessment of

the AZ which is typically assessed when PA is performed clinically, also affording a comparison of the AZ measured on imaging to our *ex vivo* assessment. Animals were euthanized immediately after ablation, having more remote time points to assess the longitudinal evolution of the AZ after treatment would have also been beneficial. Our animal model produces HT with vascularity similar to those seen in human tumors such as HCC; however, underlying liver disease will affect energy transfer and thus ablation size, the liver in this model is in a normal liver without changes of chronic liver disease or cirrhosis which is identified in many patients with HT.

CONCLUSION

The combination of embolization with PA has been studied in both pre-clinical normal livers and clinical studies, revealing an increase in the size of the AZ. We report on this combined procedure for the first time in a pre-clinical large animal orthotopic porcine liver tumor model, specifically, evaluating the embolization technique by varying the size of the particles and thus location of the embolization. Distal embolization directly affected the size of the AZ, with particle size below 300 μm generating the largest increase in the AZ.

Given our study, we hypothesize that the combination of embolization with MWA, particularly with smaller particles and multiple probes, will be able to successfully treat HT larger than 3 cm in the liver with an appropriate margin to achieve complete local cure.

Ethical approval

The research/study was approved by the Institutional Review Board at Institutional Animal Care and Use Committee (IACUC), number 103088, dated September 15, 2021.

Declaration of patient consent

Patient's consent is not required as there are no patients in this study.

Financial support and sponsorship

The study was financially supported by Ethicon Investigator-Initiated Grant.

Conflicts of interest

There are no conflicts of interest.

Use of artificial intelligence (AI)-assisted technology for manuscript preparation

The authors confirm that there was no use of artificial intelligence (AI)-assisted technology for assisting in the writing or editing of the manuscript and no images were manipulated using AI.

REFERENCES

1. Bray F, Ferlay J, Soerjomataram I, Siegel RL, Torre LA, Jemal A, 2018. Global cancer statistics 2018: GLOBOCAN estimates of incidence and mortality worldwide for 36 cancers in 185 countries. CA: a cancer journal for clinicians, 68, pp.394-424.
2. Line PD, Dueland S. Liver transplantation for secondary liver tumours: The difficult balance between survival and recurrence. J Hepatol 2020;73:1557-62.
3. Alexander ES, Ziv E. Neuroendocrine tumors: Genomics and molecular biomarkers with a focus on metastatic disease. Cancers (Basel) 2023;15:2249.
4. Senkus E, Kyriakides S, Ohno S, Penault-Llorca F, Poortmans P, Rutgers E, *et al.* Primary breast cancer: ESMO Clinical practice guidelines for diagnosis, treatment and follow-up. Ann Oncol 2015;26:v8-30.
5. Dummer R, Hauschild A, Lindenblatt N, Pentheroudakis G, Keilholz U, ESMO Guidelines Committee. Cutaneous melanoma: ESMO Clinical Practice Guidelines for diagnosis, treatment and follow-up. Ann Oncol 2015;26 Suppl 5:v126-32.
6. Van Cutsem E, Cervantes A, Adam R, Sobrero A, Van Krieken JH, Aderka D, *et al.* ESMO consensus guidelines for the management of patients with metastatic colorectal cancer. Ann Oncol 2016;27:1386-422.
7. Ruers T, Van Coevorden F, Punt CJ, Pierie JP, Borel-Rinkes I, Ledermann JA, *et al.* Local treatment of unresectable colorectal liver metastases: Results of a randomized phase II trial. J Natl Cancer Inst 2017;109:djx015.
8. Ruers T, Bleichrodt RP. Treatment of liver metastases, an update on the possibilities and results. Eur J Cancer 2002;38:1023-33.
9. Meijerink MR, Puijk RS, van Tilborg AA, Henningsen KH, Fernandez LG, Neyt M, *et al.* Radiofrequency and microwave ablation compared to systemic chemotherapy and to partial hepatectomy in the treatment of colorectal liver metastases: A systematic review and meta-analysis. Cardiovasc Intervent Radiol 2018;41:1189-204.
10. Kamarinos NV, Kaye EA, Sofocleous CT. Image-guided thermal ablation for colorectal liver metastases. Tech Vasc Interv Radiol 2020;23:100672.
11. Wolf F, Dupuy DE. Microwave ablation: Mechanism of action and devices. In: Hong K, Georgiades CS, editors. Percutaneous tumor ablation. Thieme, Strategies and Techniques; 2011. p. 27-43.
12. Brace CL, Laeseke PF, Sampson LA, Frey TM, van der Weide DW, Lee FT Jr. Microwave ablation with a single small-gauge triaxial antenna: *In vivo* porcine liver model. Radiology 2007;242:435-40.
13. Fan W, Li X, Zhang L, Jiang H, Zhang J. Comparison of microwave ablation and multipolar radiofrequency ablation *in vivo* using two internally cooled probes. AJR Am J Roentgenol 2012;198:W46-50.
14. Peng ZW, Zhang YJ, Chen MS, Xu L, Liang HH, Lin XJ, *et al*. Radiofrequency ablation with or without transcatheter arterial chemoembolization in the treatment of hepatocellular carcinoma: A prospective randomized trial. J Clin Oncol

2013;31:426-32.
15. Ginsburg M, Zivin SP, Wroblewski K, Doshi T, Vasnani RJ, Van Ha TG. Comparison of combination therapies in the management of hepatocellular carcinoma: Transarterial chemoembolization with radiofrequency ablation versus microwave ablation. J Vasc Interv Radiol 2015;26:330-41.
16. Faiella E, Calabrese A, Santucci D, de Felice C, Pusceddu C, Fior D, *et al.* combined trans-arterial embolization and ablation for the treatment of large (>3 cm) liver metastases: Review of the literature. J Clin Med 2022;11:5576.
17. Nurili F, Monette S, Michel AO, Bendet A, Basturk O, Askan G, *et al.* Transarterial embolization of liver cancer in a transgenic pig model. J Vasc Interv Radiol 2021;32:510-7.e3.
18. Reig M, Forner A, Rimola J, Ferrer-Fàbrega J, Burrel M, Garcia-Criado Á, *et al.* BCLC strategy for prognosis prediction and treatment recommendation: The 2022 update. J Hepatol 2022;76:681-93.
19. Shady W, Petre EN, Gonen M, Erinjeri JP, Brown KT, Covey AM, *et al.* Percutaneous radiofrequency ablation of colorectal cancer liver metastases: Factors affecting outcomes-A 10-year experience at a single center. Radiology 2016;278:601-11.
20. Calandri M, Yamashita S, Gazzera C, Fonio P, Veltri A, Bustreo S, *et al.* Ablation of colorectal liver metastasis: Interaction of ablation margins and RAS mutation profiling on local tumour progression-free survival. Eur Radiol 2018;28:2727-34.
21. Han K, Kim JH, Yang SG, Park SH, Choi HK, Chun SY, *et al.* A single-center retrospective analysis of periprocedural variables affecting local tumor progression after radiofrequency ablation of colorectal cancer liver metastases. Radiology 2021;298:212-8.
22. Fang Y, Chen W, Liang X, Li D, Lou H, Chen R, *et al.* Comparison of long-term effectiveness and complications of radiofrequency ablation with hepatectomy for small hepatocellular carcinoma. J Gastroenterol Hepatol 2014; 29:193-200.
23. Winokur RS, Du JY, Pua BB, Talenfeld AD, Sista AK, Schiffman MA, *et al.* Characterization of *in vivo* ablation zones following percutaneous microwave ablation of the liver with two commercially available devices: Are manufacturer published reference values useful? J Vasc Interv Radiol 2014;25:1939-46.e1.
24. Schramm W, Yang D, Haemmerich D. Contribution of direct heating, thermal conduction and perfusion during radiofrequency and microwave ablation. In: 2006 International conference of the IEEE engineering in medicine and biology society. IEEE; 2006.
25. Takamura M, Murakami T, Shibata T, Ishida T, Niinobu T, Kawata S, *et al.* Microwave coagulation therapy with interruption of hepatic blood inor outflow: An experimental study. J Vasc Interv Radiol 2001;12:619-22.
26. Chung H, Kudo M, Minami Y, Kawasaki T. Radiofrequency ablation combined with reduction of hepatic blood flow: Effect of Lipiodol on coagulation diameter and ablation time in normal pig liver. Hepatogastroenterology 2007;54:701-4.
27. Morimoto M, Numata K, Nozawa A, Kondo M, Nozaki A, Nakano M, *et al.* Radiofrequency ablation of the liver: Extended effect of transcatheter arterial embolization with iodized oil and gelatin sponge on histopathologic changes during follow-up in a pig model. J Vasc Interv Radiol 2010;21:1716-24.
28. Nakai M, Sato M, Sahara S, Kawai N, Tanihata H, Kimura M, *et al.* Radiofrequency ablation in a porcine liver model: Effects of transcatheter arterial embolization with iodized oil on ablation time, maximum output, and coagulation diameter as well as angiographic characteristics. World J Gastroenterol 2007;13:2841-5.
29. Sugimori K, Nozawa A, Morimoto M, Shirato K, Kokawa A, Saito T, *et al.* Extension of radiofrequency ablation of the liver by transcatheter arterial embolization with iodized oil and gelatin sponge: Results in a pig model. J Vasc Interv Radiol 2005;16:849-56.
30. Tanaka T, Isfort P, Braunschweig T, Westphal S, Woitok A, Penzkofer T, *et al.* Superselective particle embolization enhances efficacy of radiofrequency ablation: Effects of particle size and sequence of action. Cardiovasc Intervent Radiol 2013;36:773-82.
31. Shibata T, Niinobu T, Ogata N. Comparison of the effects of *in-vivo* thermal ablation of pig liver by microwave and radiofrequency coagulation. J Hepatobiliary Pancreat Surg 2000;7:592-8.
32. Knavel EM, Green CM, Gendron-Fitzpatrick A, Brace CL, Laeseke PF. Combination therapies: Quantifying the effects of transarterial embolization on microwave ablation zones. J Vasc Interv Radiol 2018;29:1050-6.

How to cite this article: Rice SL. Berry-Tony S, Benjamin J, Gómez Muñoz F, Alnablsi M, Beets-Tan R. Percutaneous microwave ablation of a transgenic large animal porcine liver tumor model after intra-arterial embolization. Am J Interv Radiol. 2024;8:19. doi: 10.25259/AJIR_36_2024